

## Supplementary Information

### Accelerated ageing of silicone rubber and XLPE used in HV cable accessories: a thermomechanical analysis

Oscar Kayanja<sup>1</sup>, Emre Kantar<sup>2</sup>, Svein M. Hellesø<sup>2</sup>, Julia Glaum<sup>1</sup>, Sverre Hvidsten<sup>2</sup>,  
Mari-Ann Einarsrud<sup>1\*</sup>

<sup>1</sup> Department of Materials Science and Engineering  
NTNU Norwegian University of Science and Technology  
Trondheim, Norway

<sup>2</sup> Electric Power Technology  
SINTEF Energy Research  
Trondheim, Norway

\*Corresponding author: Mari-Ann Einarsrud (mari-ann.einarsrud@ntnu.no)

#### Hardness

Shore A hardness of the hard, soft and semiconducting SiR is presented in Fig. S1.

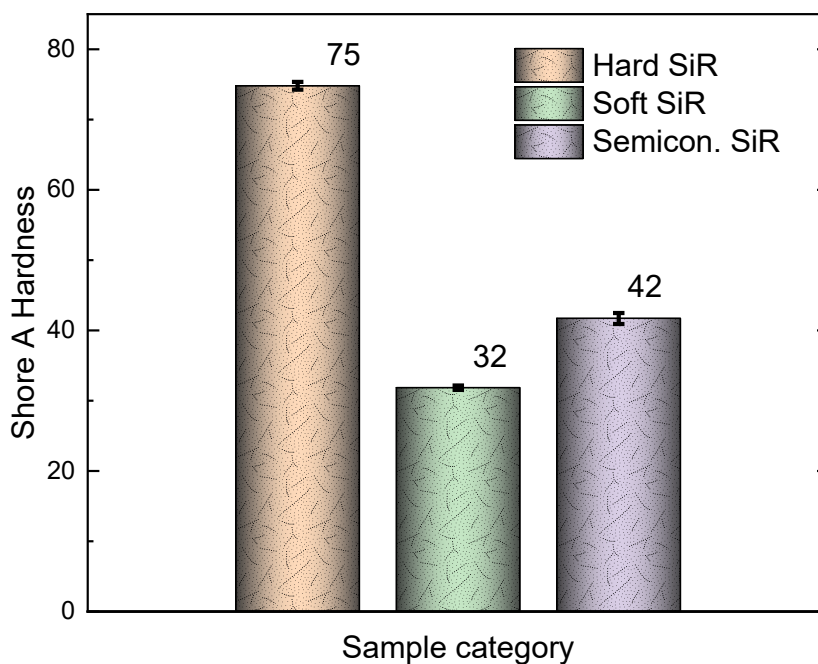


**Fig. S1.** Shore A hardness of hard, soft and semiconducting SiR samples.

## Thermomechanical cycling

The results from the thermomechanical cycling for the first and last two cycles are presented in Figs. S2 and S3. The SiR materials experienced an expansion and contraction during the ageing process arising from the oscillating temperature. The temperature profile aligned with the standard force profile, with negligible lag on both heating and cooling events during the thermomechanical cycling.

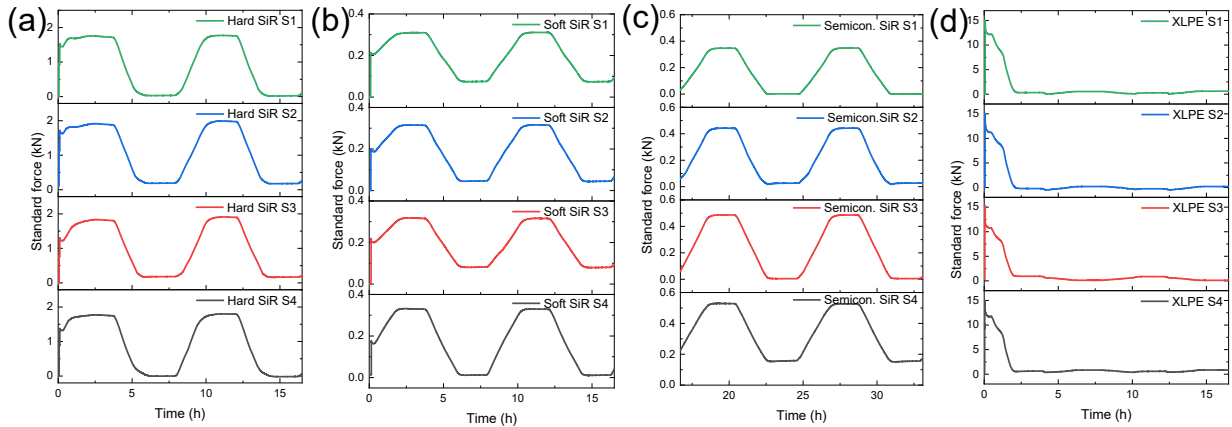


**Fig. S2.** First two cycles of standard force vs time during thermomechanical cycling for (a) hard, (b) soft, (c) semicon. SiR and (d) XLPE samples subjected to thermomechanical cycling.

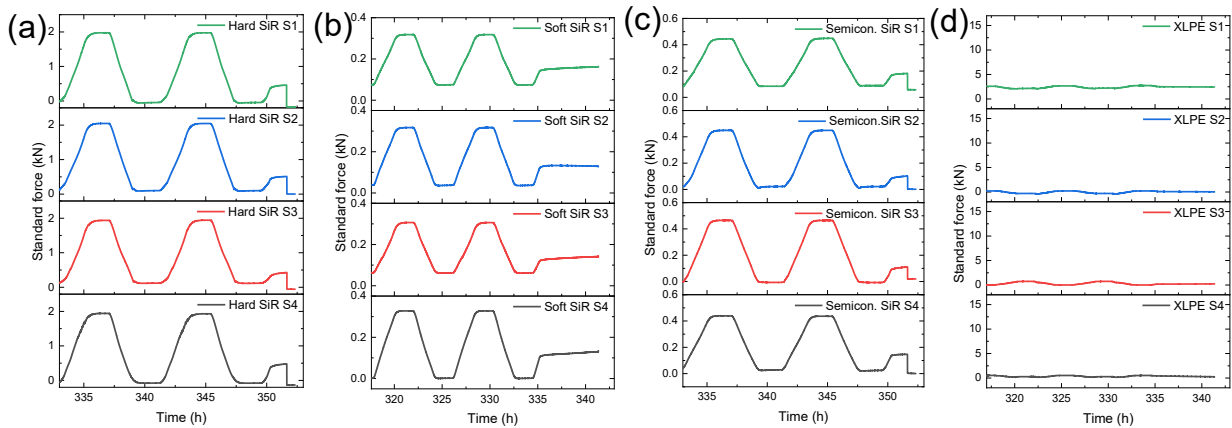


**Fig. S3.** Last two cycles of standard force vs time during thermomechanical cycling for (a) hard, (b) soft, (c) semicon. SiR and (d) XLPE samples subjected to similar thermomechanical cycling conditions.

## Post-ageing cyclic compression analysis

Cyclic size reductions at different strain levels indicated that different materials responded variably with a Mullins effect as shown in Fig. S4. By using the same strain rate for five cycles during the post-ageing cyclic compression analysis, the relative indentation force for both hard SiR and XLPE declined as shown in Fig. S5. However, for soft and semiconductive SiR, an increase in relative indentation force was observed.

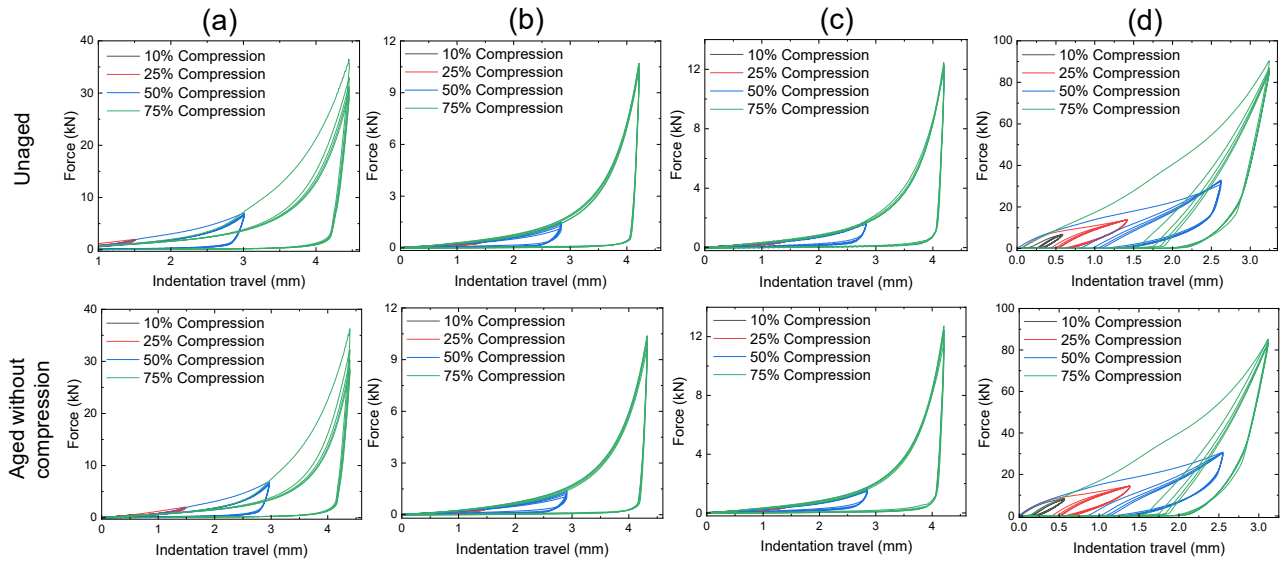


**Fig. S4.** Material response for unaged and unaged samples without compression to cyclic compression at different height reductions for (a) hard SiR, (b) soft SiR, (c) semiconductive SiR and (d) XLPE samples. A loading speed of 10 mm/min corresponding to strain rate of  $0.0278 \text{ s}^{-1}$  was used.

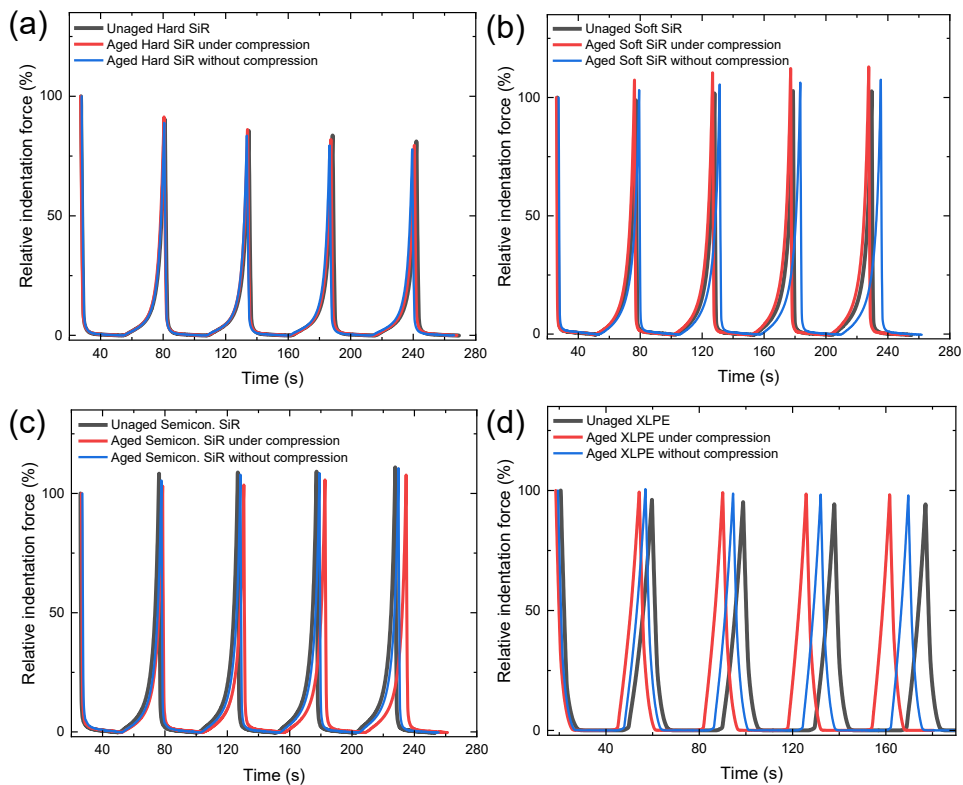


**Fig. S5.** Variation of relative indentation force with respect to time for the last cycle of 75 % height reduction for (a) hard SiR, (b) soft SiR, (c) semiconducting SiR and (d) XLPE samples.

### Changes in mass and thickness of the samples

An increase in the mass was observed for aged SiR samples after the thermomechanical cycling possibly linked to the silicone oil diffusing into the SiR material bulk (Fig. S6 (a)). A mass increase for aged XLPE was not decisively detected. A decrease in thickness was observed for all materials aged under compression, whereas a slight increase in sample thickness was observed in samples aged

without compression as shown in Fig. S6 (b). The plot of percentage change in mass as presented in Fig. S7 (a) revealed how SiR samples aged under compression had a significant increase in mass whereas those aged without compression had minimal increase in mass. Fig. S7 (b) presenting the percentage change in thickness showed how samples aged under compression had a reduction in thickness whereas those aged without compression had a slight increase in thickness.

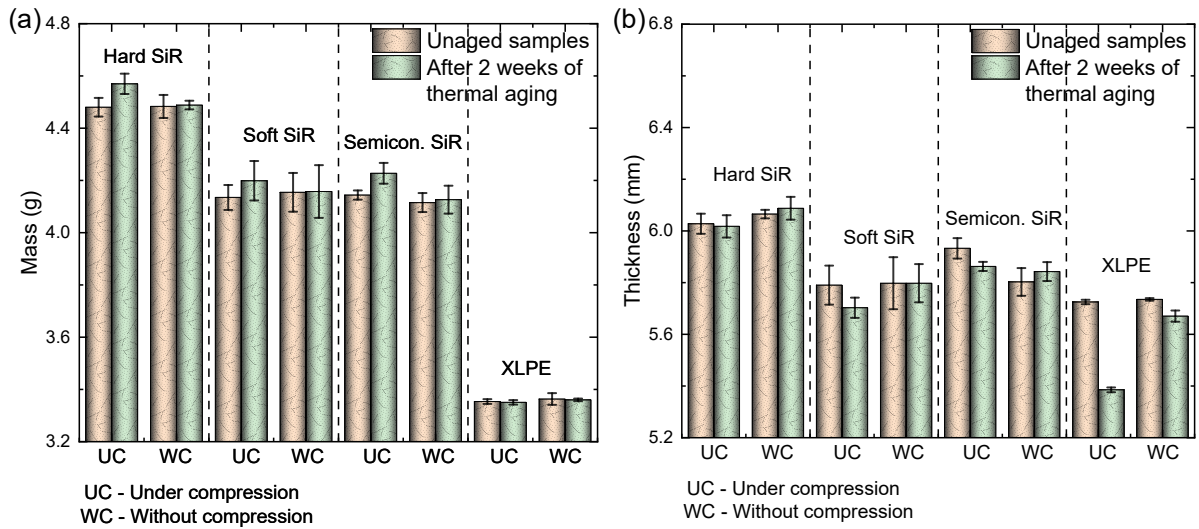


**Fig. S6.** Variation in sample (a) mass and (b) thickness before and after accelerated ageing.

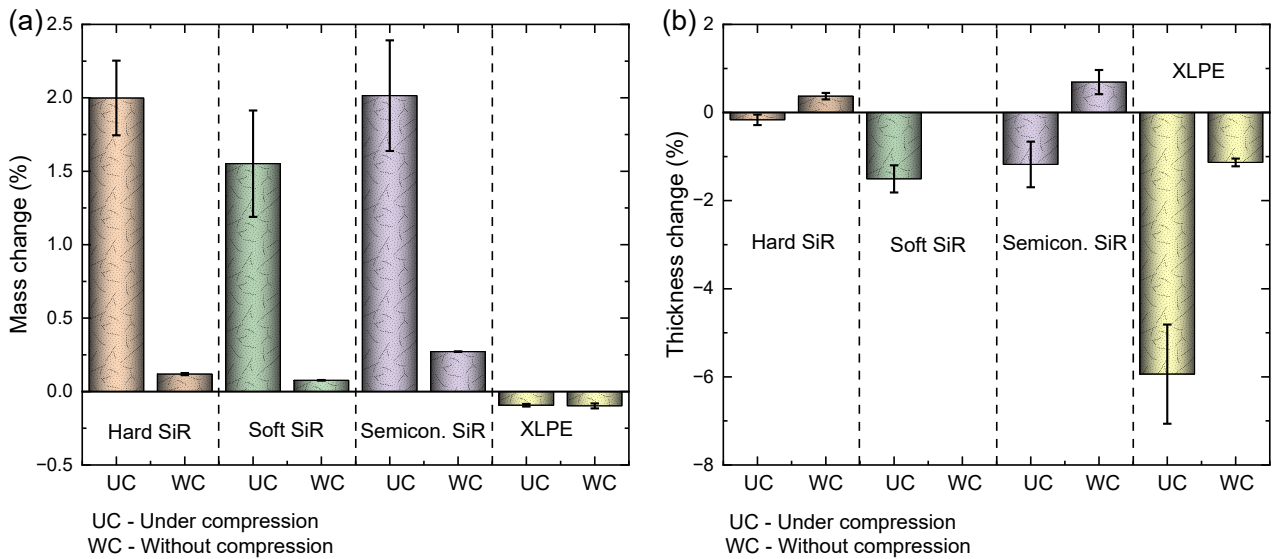


**Fig. S7.** Percentage change in (a) mass and (b) thickness for aged SiR and XLPE samples after accelerated ageing.

### Morphology of sample surfaces

Appearance of sample surfaces under a scanning electron microscope, before and after the ageing process were as shown in Fig. S8.

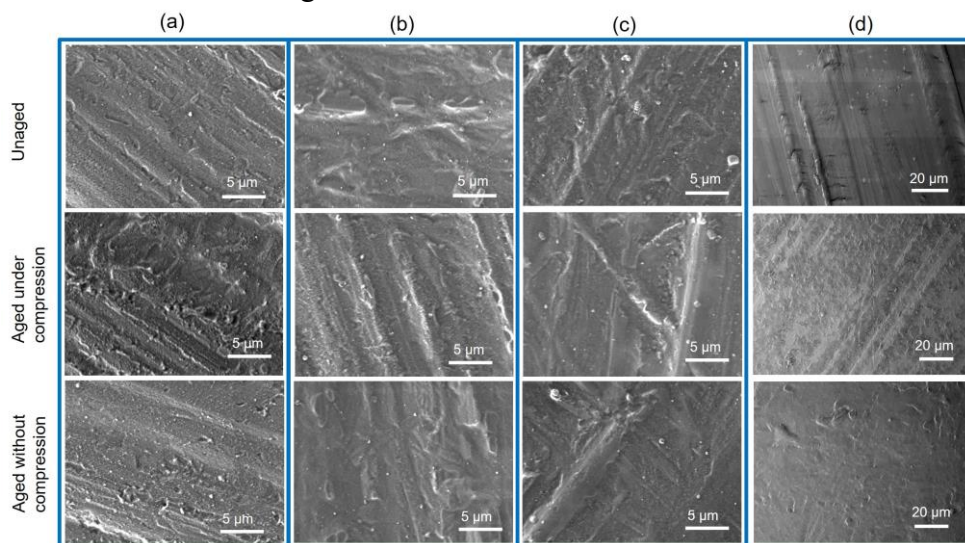


**Fig. S8.** SEM images of the top surface of (a) hard SiR (b) soft SiR, (c) semiconductive SiR and (d) XLPE samples.

### Thermal properties of the materials

DSC analysis of the different materials from -100 to 200 °C are presented in Fig. S9. The temperature range (grey shadow) of the accelerated ageing procedure did not include any thermal events for the SiR-based materials. However, for XLPE, a thermal event at 110 °C on heating due to partial crystallisation and at 91 °C on cooling due to partial conversion to an amorphous phase are observed<sup>1-3</sup>. No significant changes in the DSC data were observed for the materials after the accelerated ageing.

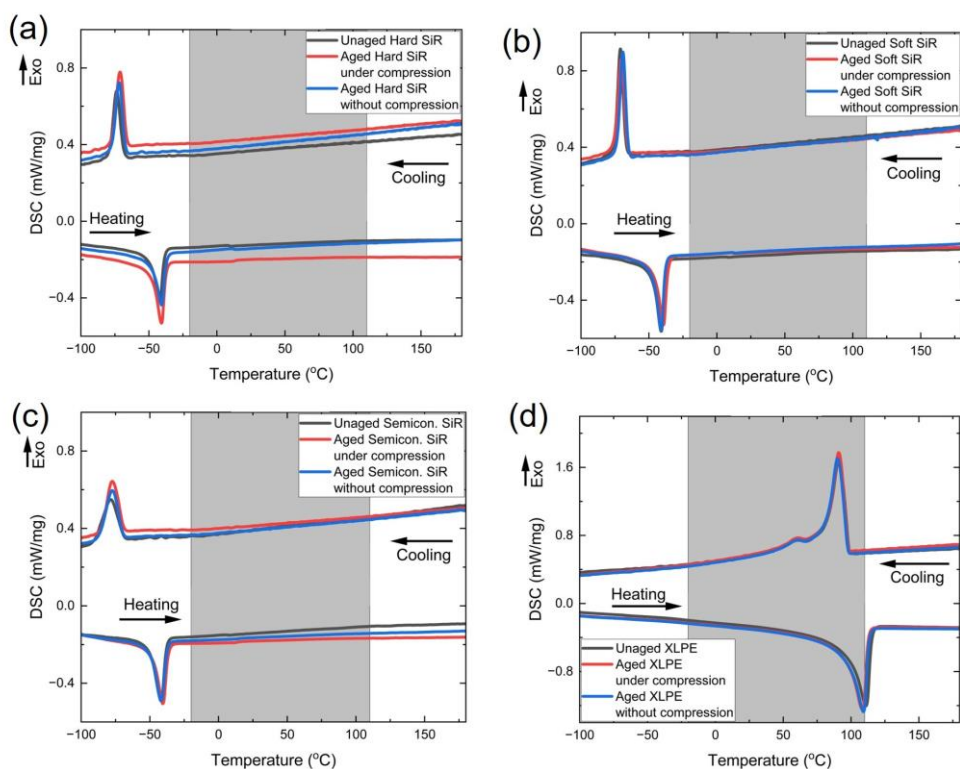


**Fig. S9.** DSC data for unaged and aged (a) hard SiR, (b) soft SiR, (c) semiconductive SiR and (d) XLPE.

Thermogravimetric analyses of the different materials are provided in Fig. S10. No significant changes in the mass of the materials are observed in the temperature range used for accelerated ageing.

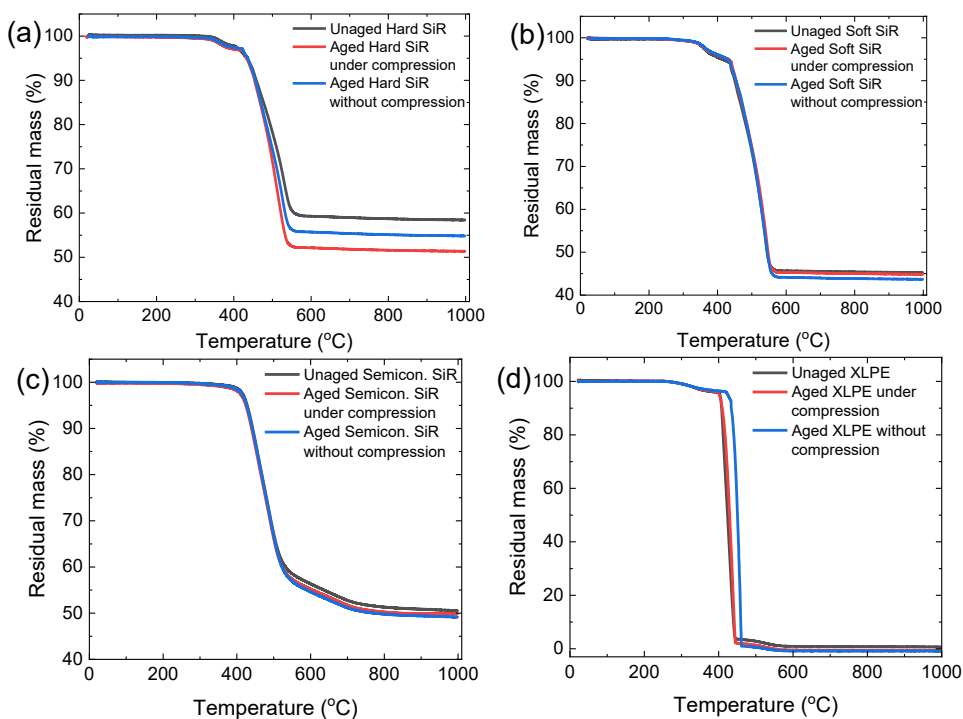


**Fig. S10.** TGA analysis for unaged and aged (a) hard SiR, (b) soft SiR, (c) semiconductive SiR and (d) XLPE heated under synthetic air using a heating rate of 10 K/min.

### Changes in physical appearance

Photos of the samples before and after the accelerated ageing are presented in Fig. S11. In transparent polymeric materials, the yellowing effect has been found to be intensified by thermal degradation<sup>4</sup>.

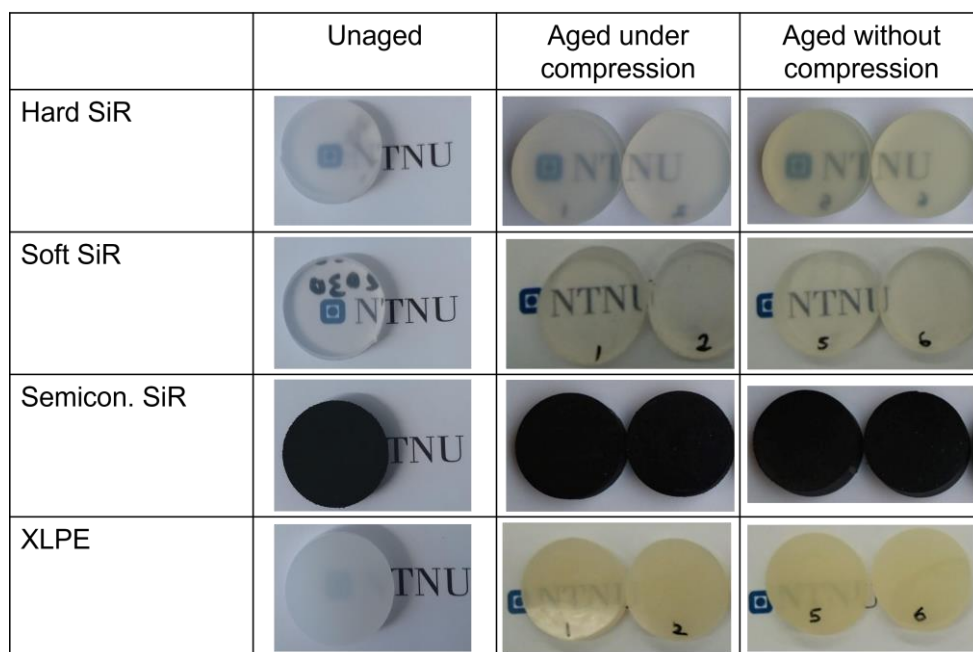


**Fig. S11.** Photos of the SiR-based and XLPE samples before and after accelerated ageing.

### Infrared spectroscopy

Comparison of FTIR spectra of unaged and aged SiR, indicates that the polymerised molecules of SiR materials were very stable to the ageing and there was no change in the main functional groups of the polymeric material as shown in Fig. S12. This has been consistent with results in literature which report minimal to no changes in the functional groups of silicone rubber materials upon application of an accelerated ageing at temperature up to 195, 47.3 and 90 °C respectively<sup>5-7</sup>. The three characteristic bands at 803, 1022, and 1100 cm<sup>-1</sup> in aged XLPE samples are due to silicone oil diffusing into the material.

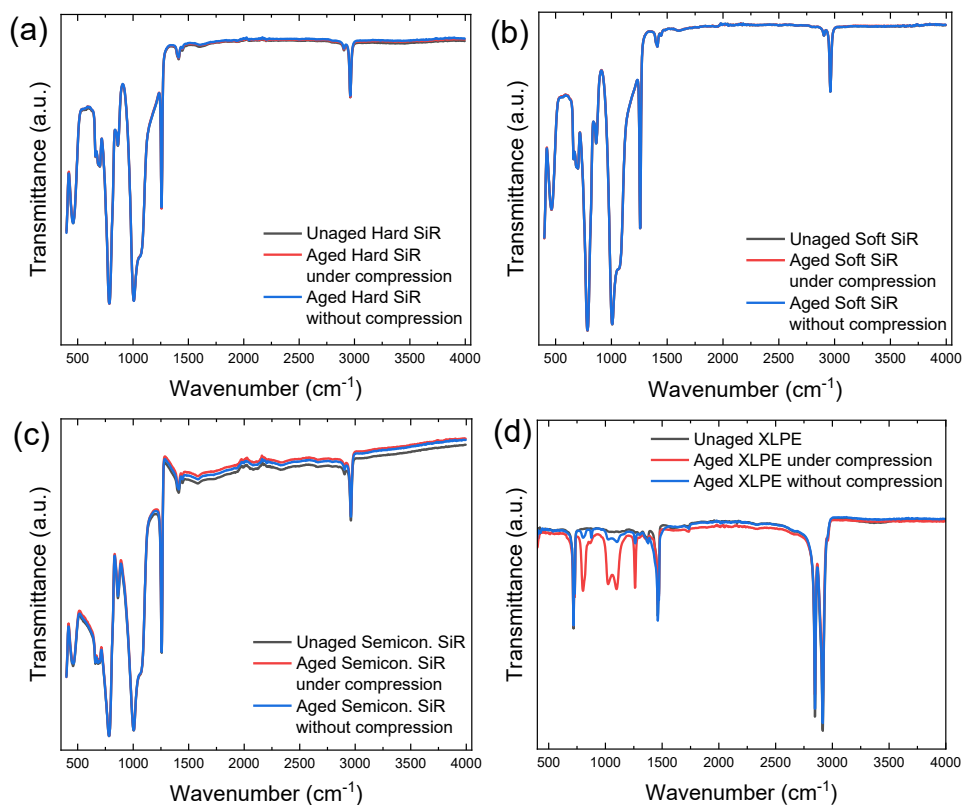


**Fig. S12.** FTIR spectra for unaged and aged (a) hard SiR, (b) soft SiR (c) semicon. SiR and (d) XLPE samples.

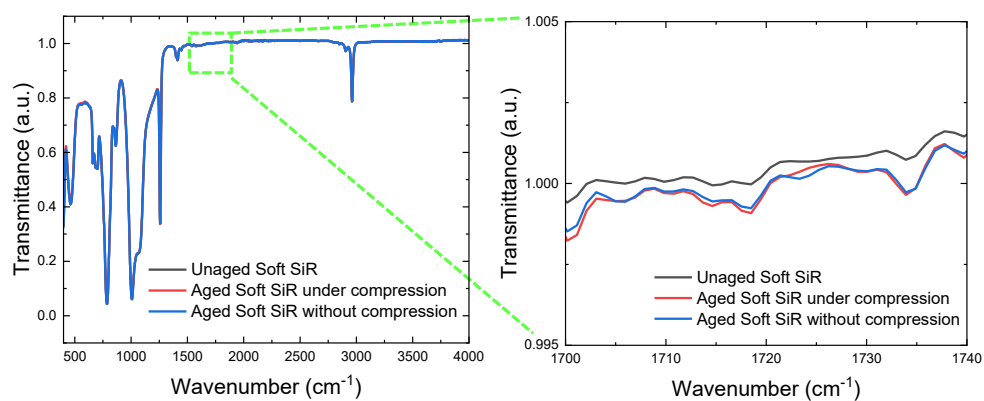


**Fig. S13.** FTIR spectra for unaged and aged soft SiR expanded at wavelengths where carboxyl and ketone groups are likely to appear as a result of oxidation.

## References

1. C. Blivet, J. F. Larché, Y. Israël, P. O. Bussiére and J. L. Gardette, Thermal oxidation of cross-linked PE and EPR used as insulation materials: Multi-scale correlation over a wide range of temperatures, *Polym. Test.*, 2021, **93**, 1–10.
2. L. Boukezzi, A. Boubakeur, C. Laurent and M. Lallouani, DSC study of artificial thermal aging of XLPE insulation cables, *2007 Int. Conf. Solid Dielectr. ICSD*, 2007, 146–149.
3. Z. Yang, H. Peng, W. Wang and T. Liu, Oxidation and Crosslinking Processes During Thermal Aging of Low-Density Polyethylene Films, *J. Appl. Polym. Sci.*, 2011, 5200–5208.

4. S. Yoon, H. Son, H. Ko and J. Kim, Analysis of yellowing phenomenon caused by electrical and thermal degradation in the interface of cross-linked polyethylene cable joints, *IET Sci. Meas. Technol.*, 2022, **16**, 503–511.
5. S. Kashi, R. Varley, M. De Souza, S. Al-Assafi, A. Di Pietro, C. de Lavigne and B. Fox, Mechanical, Thermal, and Morphological Behavior of Silicone Rubber during Accelerated Aging, *Polym. - Plast. Technol. Eng.*, 2018, **57**, 1687–1696.
6. A. Rashid, J. Saleem, M. Amin and S. M. Ali, Long-term aging characteristics of co-filled nano-silica and micro-ATH in HTV silicone rubber composite insulators, *Polym. Polym. Compos.*, 2021, **29**, 40–56.
7. C. Wu, Z. Miao, X. Wang, Y. Zhang, Z. Chen and Y. Yang, The Effect of High-low Temperature Cycle Ageing on Mechanical Properties of Silicone Rubber under Tensile State, *2023 IEEE 4th Int. Conf. Electr. Mater. Power Equipment, ICEMPE 2023*, 2023, 1–4.